ORIGINAL ARTICLE

Molecular Genetics & Genomic Medicine
Open Access
WILEY

Structural analysis of pathogenic missense mutations in *GABRA2* and identification of a novel de novo variant in the desensitization gate

Alba Sanchis-Juan[1,2] (ID) | Marcia A. Hasenahuer[3,4] | James A. Baker[3] | Amy McTague[5] | Katy Barwick[5] | Manju A. Kurian[5] | Sofia T. Duarte[6] | NIHR BioResource | Keren J. Carss[1,2] | Janet Thornton[3] | F. Lucy Raymond[2,4]

[1]Department of Haematology, University of Cambridge, NHS Blood and Transplant Centre, Cambridge, UK

[2]NIHR BioResource, Cambridge University Hospitals NHS Foundation Trust, Cambridge Biomedical Campus, Cambridge, UK

[3]European Molecular Biology Laboratory, European Bioinformatics Institute, Wellcome Genome Campus, Hinxton, Cambridge, UK

[4]Department of Medical Genetics, Cambridge Institute for Medical Research, University of Cambridge, Cambridge, UK

[5]Developmental Neurosciences, Great Ormond Street Institute of Child Health, University College London, London, UK

[6]Hospital Dona Estefânia, Centro Hospitalar de Lisboa Central, Lisbon, Portugal

Correspondence
F. Lucy Raymond, NIHR BioResource, Cambridge University Hospitals NHS Foundation Trust, Cambridge Biomedical Campus, Cambridge CB2 0QQ, UK.
Email: flr24@cam.ac.uk

Funding information
This work was supported by the National Institute for Health Research England (NIHR) for the NIHR BioResource project (grant number RG65966) and the Cambridge Biomedical Research Centre.

Abstract

Background: Cys-loop receptors control neuronal excitability in the brain and their dysfunction results in numerous neurological disorders. Recently, six missense variants in *GABRA2*, a member of this family, have been associated with early infantile epileptic encephalopathy (EIEE). We identified a novel de novo missense variant in *GABRA2* in a patient with EIEE and performed protein structural analysis of the seven variants.

Methods: The novel variant was identified by trio whole-genome sequencing. We performed protein structural analysis of the seven variants, and compared them to previously reported pathogenic mutations at equivalent positions in other Cys-loop receptors. Additionally, we studied the distribution of disease-associated variants in the transmembrane helices of these proteins.

Results: The seven variants are in the transmembrane domain, either close to the desensitization gate, the activation gate, or in inter-subunit interfaces. Six of them have pathogenic mutations at equivalent positions in other Cys-loop receptors, emphasizing the importance of these residues. Also, pathogenic mutations are more common in the pore-lining helix, consistent with this region being highly constrained for variation in control populations.

Conclusion: Our study reports a novel pathogenic variant in *GABRA2*, characterizes the regions where pathogenic mutations are in the transmembrane helices, and underscores the value of considering sequence, evolutionary, and structural information as a strategy for variant interpretation of novel missense mutations.

KEYWORDS
Cys-loop receptor, epileptic encephalopathy, *GABRA2*, protein structural analysis, whole-genome sequencing

1 | INTRODUCTION

The dynamic partnership between excitatory principal cells and inhibitory interneurons is essential for proper brain function and needs to be maintained to avoid pathological consequences. Cys-loop ligand-gated ion channels are receptors activated by neurotransmitters and play an important role in the development and activity of the central and peripheral nervous systems (Thompson, Lester, & Lummis, 2010). These receptors mediate excitatory and inhibitory synaptic transmissions depending on the distribution of ions at either side of the membrane and the membrane potential of the cell. There are two broad classifications of Cys-loop receptors, each with different electrophysiological properties: firstly, cation-selective receptors, corresponding to nicotinic acetylcholine (nACh), serotonin (5-HT$_3$), and zinc-activated receptors and secondly, anion-selective members, that include glycine (Gly) receptor and γ-aminobutyric acid receptors type A (GABA$_A$) and C (GABA$_C$) (Lester, Dibas, Dahan, Leite, & Dougherty, 2004; Thompson et al., 2010).

Cys-loop receptors are pentameric channels formed by five chains, each comprising an extracellular domain (where the ligand binds) and a transmembrane (TM) domain consisting of four TM helices (TMH), M1 to M4 (Thompson et al., 2010). The pentamers can be assembled from different gene products that encode different subunits, but all belong to the same type of receptors. For example, for the Cl⁻-selective GABA$_A$ receptors (GABA$_A$R), there are 19 genes encoding different subunits (α1-α6, β1-β3, γ1-γ3, ρ1-ρ3, δ, ε, π, θ) (Gonzalez-Nunez, 2015; D. D. Wang & Kriegstein, 2009), and the most abundant complex in adult human receptors is a combination of two α, two β, and one γ subunit (Sigel & Steinmann, 2012). Cys-loop receptors are conserved in humans and across species (Nys, Kesters, & Ulens, 2013; Ortells & Lunt, 1995). Dysfunctions of these receptors demonstrate a critical role in neurological development. Pathogenic variants in genes encoding receptors of nACh (*CHRNA2, CHRNA4,* and *CHRNB2*) and GABA$_A$ (*GABRA1, GABRB1, GABRB2, GABRB3, GABRG2,* and *GABBR2*) have previously been associated with human epilepsy (Shinichi Hirose, 2014), and mutations in Gly receptors (*GLRA1* and *GLRB*) cause hyperekplexia (Al-Owain et al., 2012; Shiang et al., 1993).

For many years, *GABRA2* (MIM: 137,140), that encodes for the GABA$_A$R subunit α2 (GABA$_A$R α2), remained as a candidate gene for epilepsy. Multiple genome-wide association studies identified noncoding single-nucleotide polymorphisms in *GABRA2* associated with increased risk for epilepsy (International League Against Epilepsy Consortium on Complex Epilepsies, 2014, 2018), as well as alcohol dependence and brain oscillations (Edenberg et al., 2004; Strac et al., 2015). Also, decreased expression of *GABRA2* in *Scn1a* ± mice served as a model of Dravet syndrome (Follwaczny et al., 2017; Hawkins, Zachwieja, Miller,

Anderson, & Kearney, 2016), and increased expression observed in Pumilio-2–deficient mice resulted in enhanced seizure susceptibility and the manifestation of epilepsy in the hippocampus (Follwaczny et al., 2017). *GABRA2* is highly expressed in the hippocampus, especially in early development, and is localized to the cell soma to mediate synaptic transmission (Prenosil et al., 2006; Tian, Chen, Cross, & Edenberg, 2005). Recently, six missense variants in *GABRA2* have been reported to cause early infantile epileptic encephalopathy (EIEE) (Butler et al., 2018; Maljevic et al., 2019; Orenstein et al., 2018): five were de novo and one was present in two affected siblings, inherited from a father who also presented the variant at low level in blood, indicating mosaicism.

Here, we describe the seventh variant in *GABRA2* to be reported as de novo in an individual with EIEE identified by whole-genome sequencing (WGS). We perform protein structural mapping and analysis of all the seven variants in the GABA$_A$R α2 and investigate the effect of the novel variant in the protein. We analyze the presence of variants in equivalent positions in other members of the Cys-loop receptor family and compare their reported effect. Furthermore, because the seven variants cluster in the TM domain, we also analyze the distribution of previously reported pathogenic variants of the Cys-loop receptors. Our results demonstrate the utility of performing variant interpretation by gathering together sequence, evolutionary, and structural information from homologous Cys-loop receptors to facilitate the characterization of novel candidate missense variants.

2 | MATERIALS AND METHODS

2.1 | Ethical compliance

The proband and both unaffected parents were recruited to the NIHR BioResource research study. The study was approved by the East of England Cambridge South national institutional review board (13/EE/0325). The research conforms with the principles of the Declaration of Helsinki. All participants provided written informed consent to participate in the study.

2.2 | Genomic analysis

WGS was performed on DNA extracted from whole blood at 30x coverage using Illumina HiSeq X Ten system (Illumina, Inc., San Diego, CA, USA) with 150bp paired-end reads. Reads were aligned to the human genome of reference GRCh37 using Isaac Aligner, and single-nucleotide variants and indels were called with both Isaac Variant Caller (Raczy et al., 2013) and Platypus (http://github.com/andyrimmer/Platypus). Variant annotation was performed with Variant

Effect Predictor (McLaren et al., 2016), which included allelic population frequencies from gnomAD (release 2.1.1) (Lek et al., 2016) and deleteriousness scores from CADD (Kircher et al., 2014), GERP (Davydov et al., 2010), SIFT (Ng & Henikoff, 2003), and Polyphen-2 (Adzhubei, Jordan, & Sunyaev, 2013). Structural variants were also called by Manta (Chen et al., 2016) and Canvas (Roller, Ivakhno, Lee, Royce, & Tanner, 2016) algorithms, as described previously (Carss et al., 2017; Sanchis-Juan et al., 2018). Trio analysis focused on de novo and rare biallelic variant discovery unrestricted by a gene list. Candidate variants were then confirmed by Sanger sequencing.

2.3 | Protein sequence conservation

Conservation of GABA$_A$R α2 was analyzed across the orthologue protein sequences for different model species and across the paralogue Cys-loop receptors from human. For that, the canonical protein sequences were obtained from UniProtKB (UniProt, 2019), then aligned using MAFFT (Katoh & Standley, 2013) with default parameters. Alignments were visually inspected and manually corrected using JalView (Waterhouse, Procter, Martin, Clamp, & Barton, 2009).

2.4 | GABA$_A$R structural analysis

There is no experimentally determined structure for the human GABA$_A$R α2 subunit, either in a homo- or heteropentameric complex. For the structural analysis of the previously reported and the novel variants, we obtained from Protein Data Bank (PDB) (Berman et al., 2000) the recently solved cryo-electron microscopy (cryo-EM) human heteropentameric GABA$_A$R α1β3γ2 complexes in closed (ID 6HUG, with resolution 3.1Å) and desensitized (ID 6HUP and 6I53, with resolution 3.58Å and 3.2Å, respectively) forms (D. Laverty et al., 2019; Masiulis et al., 2019). These structures were used as they represent the most abundant arrangement of adult human GABA$_A$R hetero-pentamers, which is two α subunits, two β subunits, and one γ subunit, with best resolution in PDB. Also, the variants analyzed were in the M1, M2, and M3 segments of the TM domain, and this region was observed, by paired local sequence alignment, to present 100% identical residues between human GABA$_A$R α1 and GABA$_A$R α2.

The closed-form structure was solved in complex with the pore blocker picrotoxin and the megabody Mb38 protein. The desensitized structures were captured in complex with diazepam (DZP), GABA, and megabody Mb38 for the ID 6HUP, and only with megabody Mb38 for the ID 6I53.

Structural mapping and visual inspection of the variants in these structures were performed using PyMOL (Delano,

2002). The electrostatic surface visualization was done using its APBS plugin (Baker, Sept, Joseph, Holst, & McCammon, 2001; Dolinsky et al., 2007). Residue interactions were calculated using Residue Interaction Network Generator (RING) (Martin et al., 2011) and visualized also with PyMOL.

Root-mean-square deviations (RMSD) were calculated fitting the structures (6HUG, 6HUP, and 6I53) among each other using the McLachlan algorithm (McLachlan, 1982) as implemented in the program ProFit (Martin, A.C.R., http://www.bioinf.org.uk/software/profit/) (Table S4).

2.5 | Channel pore characterization

To observe the effect of the pore-lining variants in the pore shape through the ion channel of the GABA$_A$R α1β3γ2 structures, four different configurations were considered: (a) where there was no mutated α1 subunit, (b) where the mutated α1 subunit was between β3 and γ2 (α1^{β3γ2}), (c) where the mutated α1 subunit was between β3 and β3 (α1^{β3β3}), and (d) where both α1 subunits were mutated (α1$^{β3γ2-β3β3}$). The three mutant structures for each closed and desensitized forms were generated with the *BuildModel* command of FoldX (Schymkowitz et al., 2005), with a previous minimization using *RepairPDB* of the same program. In both steps, the "*membrane*" parameter was turned on, and for *BuildModel*, 20 runs were requested. Then, for each mutant configuration, the structure with the lowest difference in free energy of unfolding ($\Delta\Delta G=\Delta G_{mutant}$-$\Delta G_{WT}$) was selected and the radii along the pore axis were calculated in steps of 3Å with PoreWalker (Pellegrini-Calace, Maiwald, & Thornton, 2009), and compared between them.

2.6 | Pathogenic variants in TMH of Cys-loop receptors

We characterized the distribution of pathogenic variants in other Cys-loop receptor proteins (Table S1). Pathogenic variants were obtained from ClinVar annotated as "Pathogenic," "Likely pathogenic," or "Pathogenic/Likely pathogenic" (accessed 31-Jan-2019) (Landrum et al., 2018), and Humsavar, annotated as "Disease" (release 13-Feb-2019, https://www.uniprot.org/docs/humsavar.txt). Pathogenic variants were mapped to UniProt canonical sequences using VarMap (Stephenson, Laskowski, Nightingale, Hurles, & Thornton, 2019). Only missense variants were considered. Duplicates between Humsavar and ClinVar were only counted once, where a duplicate was considered to be the same amino acid change at the same position in the same protein, and variants with conflicting interpretations between Humsavar and ClinVar were omitted. TRANSMEM annotation by SwissProt was used to determine TMH boundaries.

The Chi-square test from the SciPy python package (https://docs.scipy.org/doc/scipy/reference/generated/scipy.stats.chisquare.html) was used to compare the observed frequencies of variants that caused disease in M1, M2, M3, and M4 with those expected by chance.

3 | RESULTS

3.1 | Clinical evaluation

A female was born at term (41 weeks) by Cesarean section. There was no family history of disease and no consanguinity reported. At delivery, Apgar scores were 9 and 10 and her head circumference was 34 cm (25th-50th percentile). She presented at 15 months of age with nonspecific EIEE and global hypotonia. Seizures occurred during sleep, with and without fever, and were tonic with upward eye deviation, or eye and head deviation to either side. MRI performed at 19 months was normal. EEG at onset of epilepsy was normal, but later investigations showed slow and irregular background activity, without paroxysmal activity. She presented developmental delay, especially affecting language (comprehension and expression), but also behavior disturbance including hyperactivity, repetitive routines or rituals, and marked disturbance with changes in the environment. She also developed hand stereotypies (waving, finger repetitive movements). She was treated with sodium valproate and clobazam that controlled her seizures. Currently, she is 10 years old and has severe impairment of language, hand stereotypies, disruptive behavior, and repetitive movements. All routine genetic analyses were negative. Additional clinical details for this individual are compared to the previously reported cases (Maljevic et al., 2019) in Table S2.

3.2 | Identification of a novel de novo mutation in _GABRA2_

A novel de novo missense mutation was identified in _GABRA2_ at genomic position Chr4(GRCh37):g.46305494 G > A, NM_000807.2:c.839C > T, NP_000798.2:p. Pro280Leu by WGS trio analysis of DNA from both parents and the child. The variant was confirmed by Sanger sequencing (Figure S1). No other candidate variant was identified in this individual from trio analysis. The gene was observed to be constrained for loss of function (LOF) variation (with pLI = 1 and observed/expected score = 0.05) and missense variation (Z score = 3.13) in gnomAD (Lek et al., 2016), especially in the TM region and ligand-binding domain of the neurotransmitter-gated ion channel (Figure 1a and Figure S2) (Havrilla, Pedersen, Layer, & Quinlan, 2018).

Pro280 is located in M2, the second helix in the TM domain (Figure 1b,c). It is highly conserved across species (Figure 1b) and across different subunits from the GABA$_A$R family in human (Figure S3a). This variant is absent in gnomAD database (Figure 1a) and was predicted to be damaged by CADD, GERP, SIFT, and Polyphen-2 (with scores of 29.4, 5.17, 0.02 and 1, respectively).

3.3 | Structural characterization of the novel and previously reported variants in GABA$_A$R α2

Protein structural mapping of the seven variants revealed their proximity to the desensitization gate, the activation gate, or the M1-M3 inter-subunit interfaces of the receptor.

The variants at the desensitization gate are Pro280Leu and Val284Ala. This gate is defined by the region between −2' and 2' positions of the receptor and modulates the conductance and ion-selectivity, as observed in the structures of GABA$_A$ and Gly receptors (Gielen, Thomas, & Smart, 2015; Hibbs & Gouaux, 2011; Sauguet et al., 2013). Pro280 is located at the TM region of the receptor, in the N-terminal end of the M2 helix in the cytoplasmic facing leaflet (Figure 2), and corresponds to the exact −2' position. The side chains of the amino acids in this position (Pro in the case of α1-α6 and γ1-γ3 subunits, Ala in β1-β3 subunits), coming from each chain of the pentamer, altogether define the inner narrowest constriction of the pore, known as the −2' ring (Hibbs & Gouaux, 2011), as shown in Figure 2b and c. A reduction in the diameter of the pore is observed upon the introduction of this variant (Figure S4a,b). Small nonpolar amino acids (proline and alanine) are conserved at the −2' position in human GABA$_A$ and Gly anion-selective receptors (Figure 3a), suggesting the necessity of maintaining the size, shape, and absence of charge in the inner constriction of this pore for the adequate transit of anions. In contrast, in cation-selective receptors, a negatively charged amino acid (glutamate) with a longer and more flexible side chain is usually observed in position −1' (Figure S3a).

Val284, corresponds to the precise 2' position. In this case, the side chains of the amino acids in this position do not define a ring, but establish inter-subunit Van der Waals (VDW) interactions with M2 helices from the β3 subunits (Figure 2c) (Hibbs & Gouaux, 2011). Having an alanine instead of a valine at this position affects the radius of the pore differently depending on the arrangement of the different subunits and the state of the receptor (Figure S4a,c).

The variant Asn335His is near the desensitization gate, at 9.5 Å (in PDB ID 6HUP) from −2' position in α1-M2 (Pro280). Asn335 is located at the C-terminus of the M3 helix, on the inner side of the TM region, at the base of the helical
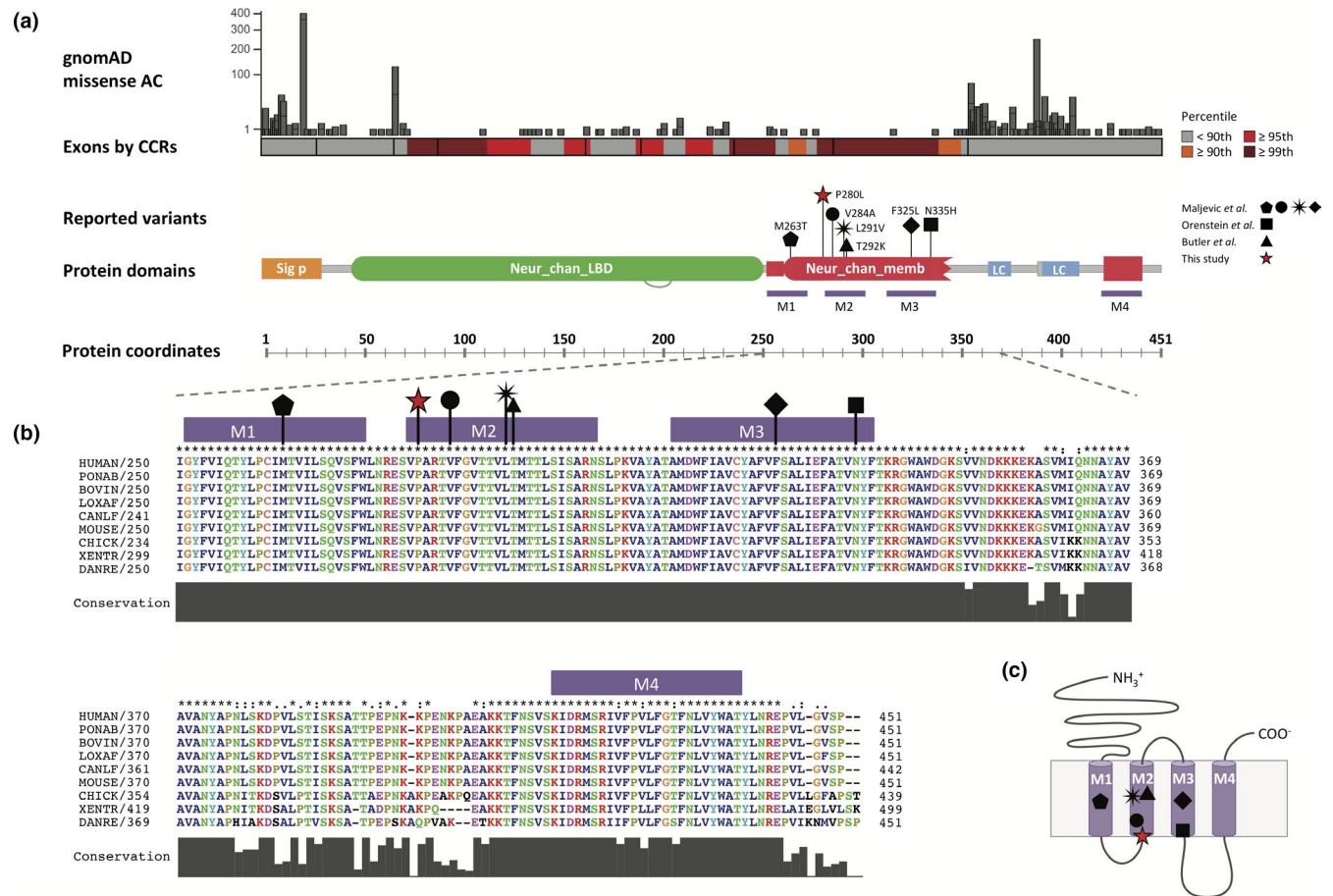
FIGURE 1 (a) Schematic diagram showing the architecture of domains in GABA_A α2. At the top are represented the allele count of missense variants followed by the constrained coding regions' percentiles (Havrilla et al., 2018), both based on gnomAD release 2.1.1. The seven variants in *GABRA2* are indicated with different symbols (triangle, square, circle, diamond, pentagon, black star, and red star), and cluster in the TM region, which is highly constrained for variation in control population (see also Supp. Figure 2a). Coordinates of the protein domains were obtained from Pfam (https://pfam.xfam.org). Sig_p = signal peptide; Neur_chan_LBD = neurotransmitter-gated ion-channel ligand-binding domain; Neur_chan_memb = neurotransmitter-gated ion-channel TM region; LC = low complexity; TM = transmembrane. (b) Alignment of the TM region of GABA_A α2 subunit across representative vertebrate species. The regions where the variants fall are evolutionarily conserved through these species. Colors are by amino acid properties. Ponab = orangutan; Bovine = cow; Loxav = elephant; Canlf = dog; Chick = chicken; Xentr = xenopus; Danre = zebrafish. (c) Schematic representation of GABA_A α2 TMH. The locations of the seven missense variants are approximate

bundle, and participates in inter- and intra-subunit interactions with residues in the M2-M3 loops of β3 and γ2 chains, including Val279 (Figure 2c). This network of contacts has been proposed to be important to stabilize the desensitized state of a GABA_AR (the homo-pentameric GLIC-GABA_R α1 chimeric receptor) (Gielen et al., 2015; Duncan Laverty et al., 2017). This stabilization could be affected by the substitution to a positively charged histidine.

The variant Leu291Val is at the activation gate, which has been defined as the ring formed by the leucines at the 9' position, and is important for the transition between opened and closed states of the ion channel (Duncan Laverty et al., 2017). The precise 9' position corresponds with Leu291 and is located in the pore-lining M2 helix of the TM domain (Figure 2b,d). Having a valine instead of a leucine at this residue increases the diameter of the pore (Figure S4a,d) and alters

the VDW interactions that define the 9' ring as well as the inter-subunit interactions with the threonines from the neighboring β3 and γ2 chains.

Thr292Lys is at the 10' position, which is adjacent to the activation gate. Thr292 is at the turn of the alpha helix that faces the inter-subunit interface, and is involved in inter- and intra-subunit VDW interactions with Thr264 in M1 of its same α1 subunit, and with the β3 subunit residues Leu287 and Leu284, being the last one part of the 9' ring of this subunit (Figure 2b,d).

The variants in M1-M3 inter-subunit interfaces are Met263Thr and Phe325Leu. Met263 is located at the middle of the M1 helix, at 13.5Å (in PDB ID 6HUP) from the 9' activation gate of β3-M2. It is involved in a network of VDW interactions with residues from the M3 helix of the neighboring β3 subunit, and it is located near the Thr264
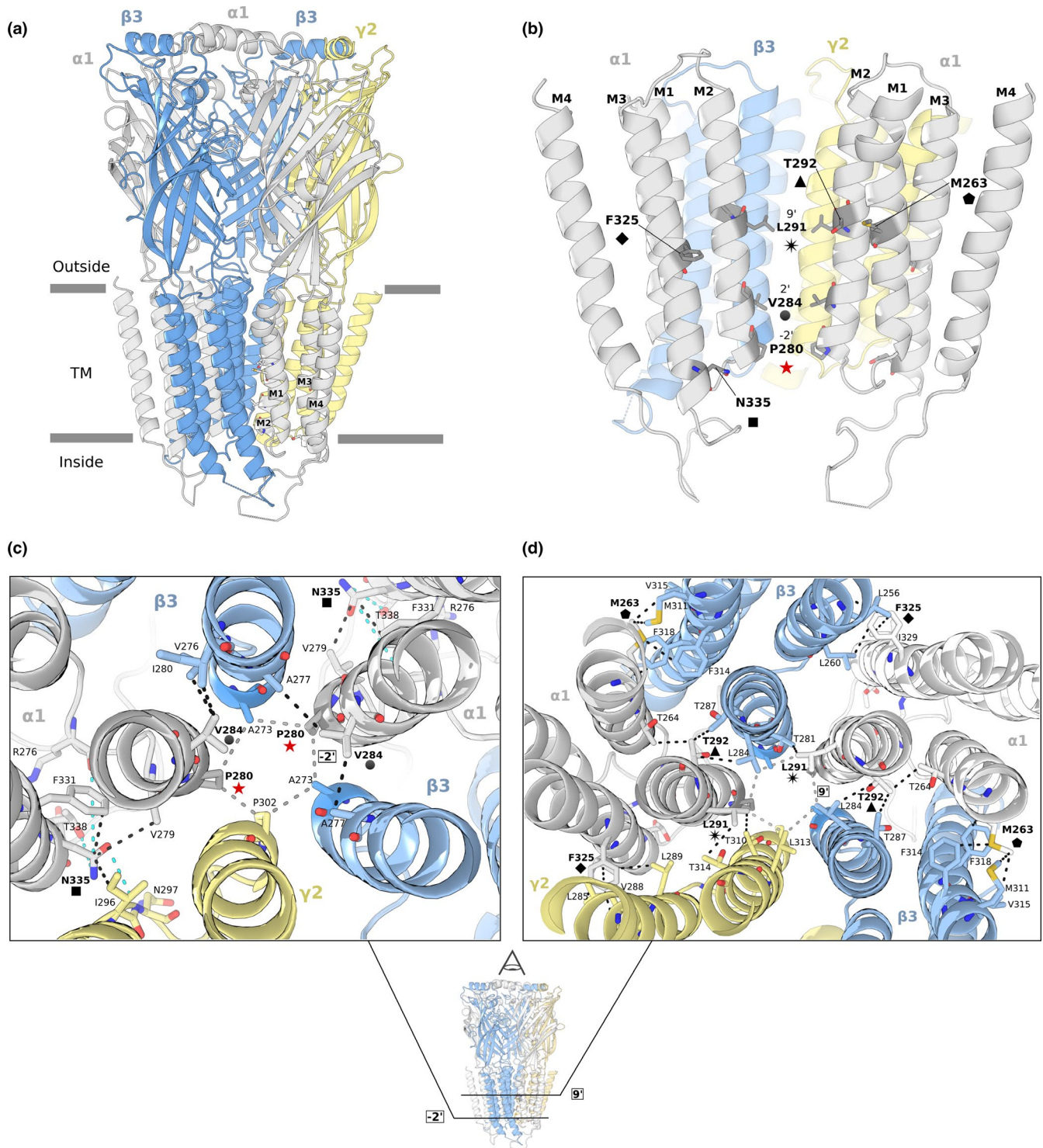
FIGURE 2 (a) The GABA$_A$ α1β3γ2 receptor in closed state. M1 to M4 helices are depicted over the homologous human GABA$_A$R α1 chain (PDB ID 6HUG). The two α1 chains are in grey, the two human β3 chains in blue, and the human γ2 in yellow, with the approximate boundaries of the TM in grey bars. (b) Side view of the transmembrane helices of the GABA$_A$ α1β3γ2 receptor in closed state. The structural location of the variants is depicted consistently using the same symbols as in Figure 1a. For a clearer view, the chain between two α1 subunits is hidden. (c) Down the pore axis view of the variants nearby the −2' ring (Pro280Leu, Val284Ala, Asn335His), and (d) the 9' ring (Met263Thr, Leu291Val, Thr291Lys, Phe325Leu). VDW interactions for the residues where the variants fall are in black dashed lines (except for the rings that are in grey) and hydrogen bonds are in cyan

residue, which interacts with the Thr292 (Figure 2b,d). Met263 is also part of the recently reported low-affinity binding site for benzodiazepines, a group of sedative

anticonvulsant drugs (Masiulis et al., 2019; Olsen, 2018; Walters, Hadley, Morris, & Amin, 2000). In the desensitized GABAA α1β3γ2 receptor bound to diazepam (DZP),

Met263 is part of the opening of the pocket to the external molecular surface and its lateral chain sulfur establishes direct interaction with the diazepine ring of DZP (Figure S5). Having a smaller threonine with a polar uncharged lateral chain instead of methionine would affect the size and shape of the entrance to this pocket and the interactions established with the benzodiazepines. It can also be observed, deeper in the pocket, that the benzene ring of DZP also interacts with Thr292.

Lastly, Phe325 is at the middle of M3 helix, at 3.7 Å (in PDB ID 6HUP) from the 9' activation gate of α1-M2. It is also involved in a network of VDW interactions with residues of M1 from either β3 or γ2 (Figure 2b,d). Some evidence points to the α1 residues Ser297 and Ala318 in the α1-M3 β3-M2 TM interface as critical for the receptor modulation by diverse anesthetic molecules (Mihic et al., 1997).

3.4 | The novel variant Pro280Leu affects the diameter of the channel pore in the desensitization gate

We introduced in silico the mutation Pro280Leu into the cryo-EM structure of GABA$_A$R α1β3γ2 closed and desensitized forms (Figure 3 and Figure S4), in the four situations: α1$_{P280}$, α1$^{β3γ2}_{P280L}$, α1$^{β3γ2-β3β3}_{P280L}$, and α1$^{β3β3}_{P280L}$. In Figure 3, only the first three are shown for simplicity.

The larger nonpolar amino acid chain of the leucine narrowed the constriction region compared to the nonmutated receptors (Figure 3d and Figure S4a,b) measuring the radius at 3 Å steps along the pore axis. The largest changes in all the situations occurred at 12 Å (−2') and 15 Å. For the desensitized structure of the receptor that has GABA and DZP, this reduction can also be observed at 18 Å (2').

FoldX stability calculations showed higher ΔΔG values, which correspond with higher destabilizing effects in the desensitized compared to the closed forms (Table S3). Also, these showed higher ΔΔG values when both α1 chains were mutated.

3.5 | Location of GABA$_A$α2 mutations is equivalent to pathogenic variants in other Cys-loop receptors

We investigated if the location of the seven variants in GABA$_A$α2 had equivalent positions also mutated and associated with disease in other Cys-loop receptors. Six of the seven variants had at least one pathogenic mutation at the equivalent or flanking position in other Cys-loop receptor genes. These variants are highlighted in the alignment of the Cys-loop receptor sequences in Figure S3b. Additional information for the variants is shown in Table 1.

The same amino acid change that we observed in *GABRA2* (Pro280Leu) was reported at the equivalent location in *GABRG2* in an individual with Dravet syndrome (NM_198903.2(*GABRG2*):p.Pro302Leu) (Hernandez et al., 2017), and a different amino acid change was observed in an individual with autosomal dominant hyperekplexia (NM_001146040.1(*GLRA1*):p.Pro278Thr) (Saul et al., 1999). Both mutations, like the Pro280Leu, were in the −2' ring of the receptors. The authors demonstrated that these mutations enhanced desensitization and reduced both the "channel open" probability and the frequency of receptor single-channel openings.

For the Met263, five pathogenic mutations in other Cys-loop receptor genes were observed to be equivalent to this exact position, and one was present in the adjacent amino acid (Aridon et al., 2006; Farnaes et al., 2017; Kodera et al., 2016; Epi, 2016). This variant is in the M1 helix of the TM domain, in the inter-subunit interface with the M3, and this region is important for the actions of potentiating neuroactive steroids (Akk et al., 2008). Functional studies of the variant equivalent to the previous amino acid in *CHRNA2* (NM_000742.3:p.Ile279Asn) showed that it increases the receptor sensitivity to the neurotransmitter, without affecting desensitization properties and channel permeability.

Three variants reported in the literature were observed in the adjacent amino acids to the Val284Ala (2') of *GABRA2* (Table 1) (Conti et al., 2015; Hamdan et al., 2017). Functional studies on the NM_000742.3(*CHRNA2*):p.Ile297Phe were consistent with the loss of function of the receptor, either by impaired channel expression onto the cell surface or by a drastic decrease in the channel open probability (Conti et al., 2015).

Variants in the leucines that form the 9' ring have been previously reported in other members of the Cys-loop receptors as associated with congenital myasthenic syndrome and hyperekplexia (Table 1) (Gomez et al., 1996; James et al., 2013). Mutations at this site are known to destabilize the closed state of the receptor and produce spontaneously active channels. Functional works on the NM_000747.2(*CHRNB1*):p.Leu285Met (9') showed reduced stability of the closed gate and abnormal channel openings even in the absence of the neurotransmitter, consistent with a receptor that is caught in the open state (Gomez et al., 1996).

The equivalent position to Thr292 in GABA$_A$ α2 has been reported as pathogenic in *GLRA1* (NM_000171.3:p.Thr290Ile) and *CHRNA4* (NM_000744.6:p.Ser284Leu) (Cho et al., 2003; S. Hirose et al., 1999; Hwang, Makita, Kurahashi, Cho, & Hirose, 2011; Kurahashi & Hirose, 2002). Expression studies of the *CHRNA4*-Ser284Leu demonstrated higher affinity to acetylcholine and faster desensitization of the receptors and is reported in multiple
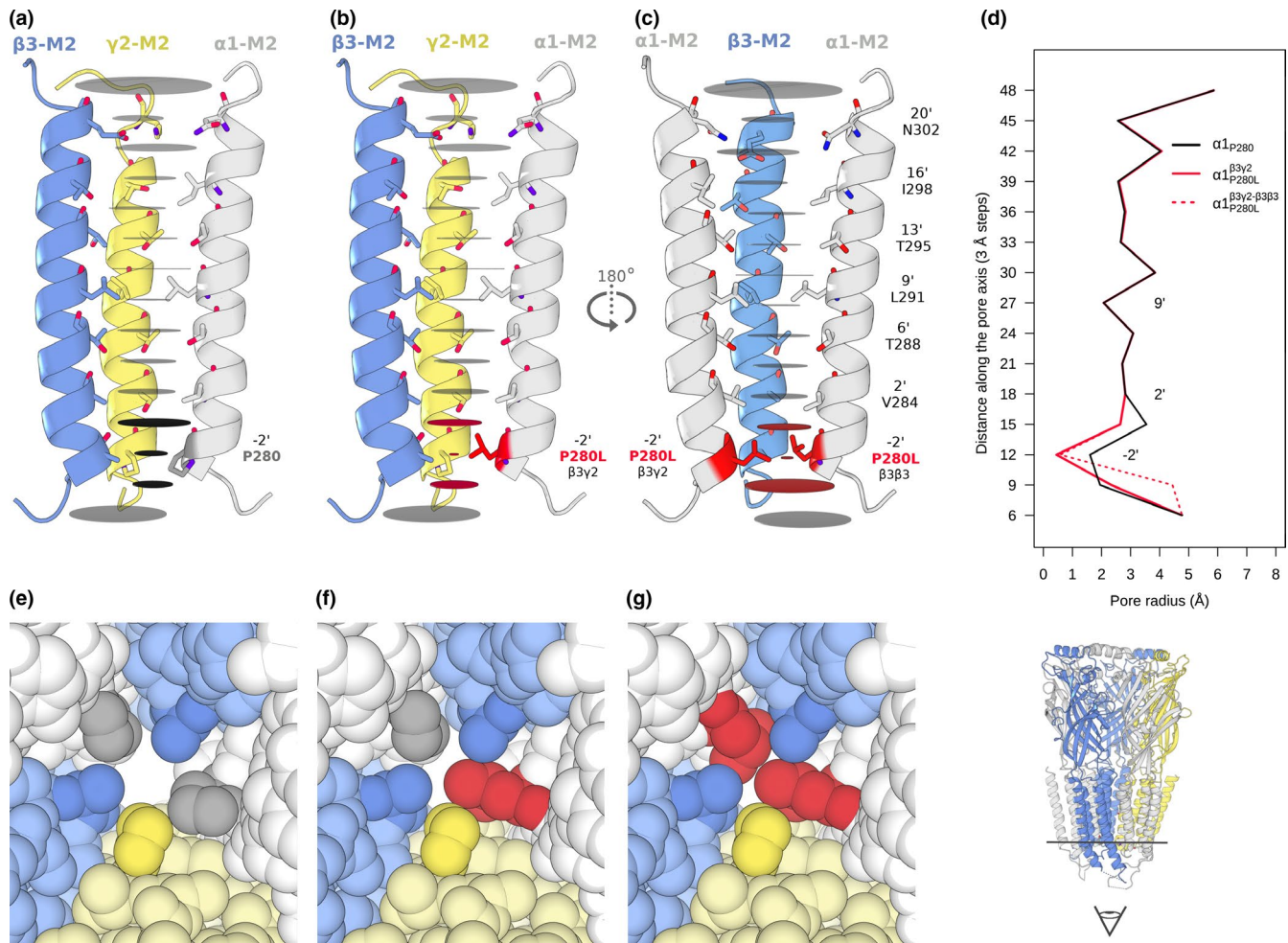
FIGURE 3 Effect of Pro280Leu in the pore radii of the GABA$_A$ α1β3γ2 receptor in its closed form. Radii profile through the TM pore axis by 3 Å steps for: (a) Nonmutant GABA$_A$ α1β3γ2 (α1$_{P280}$), (b) mutant α1 subunit is between β3γ2 (α1$^{β3γ2}_{P280L}$), and (c) both α1 subunits are mutated (α1$^{β3γ2-β3β3}_{P280L}$). M2 pore-lining residues are shown in sticks. The pore radii at each step along the pore vertical axis are represented with horizontal grey discs. The pore is narrowest in α1$_{P280}$ at the −2' position (1.60 Å), which is smaller than the Pauling ionic radius of Cl$^−$ (1.81 Å) and the radius of hydrated Cl$^−$ (3.2 Å). For clarity, only three M2 helices are represented in each situation. The steps with affected radii upon Pro280Leu are colored in red in (b) and (c). (d) Pore radius plotted as a function of longitudinal distance along the pore axis, vertically aligned to match the steps in (a), (b), and (c) panels. The biggest radii reduction can be observed at 12 Å (−2' position) from 1.60 Å in α1$_{P280}$ to: 0.58 Å (Δ=1.02 Å) in α1$^{β3γ2-β3β3}_{P280L}$ and 0.45 Å (Δ=1.15 Å) in α1$^{β3γ2}_{P280L}$. Also, reductions can be observed at 15 Å (region between −2' and 2' positions) from 3.55 Å in α1$_{P280}$ to: 2.64 Å (Δ= 0.91 Å) in α1$^{β3γ2-β3β3}_{P280L}$ and 2.64 Å (Δ= 0.91 Å) in α1$^{β3γ2}_{P280L}$. Increments in the radii are observed at 9 Å from 1.95 Å in α1$_{P280}$ to: 4.44 Å (Δ=2.49 Å) in α1$^{β3γ2-β3β3}_{P280L}$ and 2.33 Å (Δ=0.38 Å) in in α1$^{β3γ2}_{P280L}$. This step at 9 Å corresponds to the vestibule region adjacent to the −2' ring in the inner cytoplasmic side. Zoom over the inner cytoplasmic vestibule of the pore defined by the amino acids of the −2' ring for (e) nonmutant GABA$_A$ α1β3γ2, (f) mutant α1 subunit is between β3γ2 (α1$^{β3γ2}_{P280L}$), and (g) both α1 subunits are mutated (α1$^{β3γ2-β3β3}_{P280L}$). The color for each subunit chain matches the ones used in Figure 2

affected individuals (Steinlein, Hoda, Bertrand, & Bertrand, 2012).

Lastly, two variants were reported at the equivalent position to Phe325 in *GABRA2* and three were in the adjacent amino acid (Table 1). Functional studies on the variant in *CHRNA1* (NM_001039523.2:p.Val330Ile, equivalent to the adjacent Val324 in *GABRA2*) showed it affects the speed and efficiency of gating of its channel, slowing opening and increasing closing rates (H. L. Wang et al., 1999).

3.6 | Disease variants in TMH of Cys-loop receptors are most commonly found in M2

The previously reported and novel variants in *GABRA2* fall in the TMH of the ion channel. TMHs are enriched for germline disease variants compared to other regions (Dobson, Meszaros, & Tusnady, 2018). Therefore, we investigated the location of all pathogenic ClinVar and Humsavar variants reported in proteins from the Cys-loop receptors (Table S2) to contain pathogenic variants present in ClinVar and Humsavar.

TABLE 1 Details of variants in equivalent positions to the seven mutations in *GABRA2* (NM_000807.2) identified in other Cys-loop receptor genes

Mutation in GABRA2	Gene	Family	HGVSc	HGVSp	Equivalent position in GABRA2	Reference SNP	References	Source
Met263Thr	CHRNA2	nACh	NM_000742.3(CHRNA2):c.836T > A	Ile279Asn	262	rs104894063	(Aridon et al., 2006)	ClinVar; Humsavar
	GABRA1	GABA-A	NM_000806.5(GABRA1):c.788T > A	Met263Lys	263	rs796052491	–	ClinVar
	GABRA1	GABA-A	NM_000806.5(GABRA1):c.789G > A	Met263Ile	263	rs1060499553	(Farnaes et al., 2017)	ClinVar
	GABRA1	GABA-A	NM_000806.5(GABRA1):c.788T > C	Met263Thr	263	–	(Kodera et al., 2016)	Manual
	GABRB3	GABA-A	NM_000814.5(GABRB3):c.766C > G	Leu256Val	263	rs1555401942	–	ClinVar
	GABRB3	GABA-A	NM_000814.5(GABRB3):c.767T > A	Leu256Gln	263	–	(Epi, 2016)	Humsavar
Pro280Leu (−2')	GABRG2	GABA-A	NM_198903.2(GABRG2):c.905C > T	Pro302Leu	280	–	(Hernandez et al., 2017)	Manual
	GLRA1	Gly	NM_001146040.1(GLRA1):c.832C > A	Pro278Thr	280	rs121918413	(Saul et al., 1999)	ClinVar; Humsavar
Val284Ala (2')	CHRNA2	nACh	NM_000742.3(CHRNA2):c.889A > T	Ile297Phe	283	rs1554514507	(Conti et al., 2015)	ClinVar
	GABRB2	GABA-A	NM_021911.2(GABRB2):c.830T > C	Leu277Ser	285	rs1554094145	(Hamdan et al., 2017)	ClinVar
	GABRG2	GABA-A	NM_000816.3(GABRG2):c.919T > G	Leu307Val	285	rs796052509	–	ClinVar
Leu291Val (9')	CHRNB1	nACh	NM_000747.2(CHRNB1):c.853C > A	Leu285Met	291	rs137852811	(Gomez et al., 1996)	ClinVar; Humsavar
	GLRB	Gly	NM_000824.4:c.920_921ΔInsGA	Leu307Arg	291	–	(James et al., 2013)	Humsavar
	GABRA1	GABA-A	NM_000806.5(GABRA1):c.868G > A	Val290Met	290	rs796052494	–	ClinVar
	GABRB2	GABA-A	NM_021911.2(GABRB2):c.845T > C	Val282Ala	290	rs886039374	–	ClinVar
	GLRA1	Gly	NM_001146040.1(GLRA1):c.862G > A	Val288Met	290	rs121918416	(del Giudice et al., 2001)	ClinVar
Thr292Lys	GLRA1	Gly	NM_000171.3(GLRA1):c.869C > T	Thr290Ile	292	rs1064795411	–	ClinVar
	CHRNA4	nACh	NM_000744.6(CHRNA4):c.851C > T	Ser284Leu	292	rs28931591	(Cho et al., 2003; S. Hirose et al., 1999; Hwang et al., 2011; Kurahashi & Hirose, 2002)	ClinVar
Phe325Leu	CHRNB2	nACh	NM_000748.2(CHRNB2):c.923T > C	Val308Ala	324	rs281865070	–	ClinVar
	GABRA1	GABA-A	NM_000806.5(GABRA1):c.973T > C	Phe325Leu	325	rs1064794681	–	ClinVar
	GABRB2	GABA-A	NM_021911.2(GABRB2):c.946G > A	Val316Ile	324	rs1554093884	–	ClinVar
	GABRB2	GABA-A	NM_021911.2(GABRB2):c.950_951del TCinsCA	Phe317Ser	325	rs1554093882	–	ClinVar
	CHRNA1	nACh	NM_001039523.2(CHRNA1):c.988G > A	Val330Ile	324	rs137852804	(H. L. Wang et al., 1999)	ClinVar

About 265 variants were within the TMH, of which 86 were annotated as disease-causing. Three hundred and ninety-eight variants were found in the TMH including ± 5 flanking residues, of which 122 were annotated as disease-causing, being 82 from ClinVar, 11 from Humsavar, and 29 from both. Within the TMH region, disease variants were more commonly found in, or in close proximity to, M2 than other TMH. Thirty-nine disease variants were observed in the M2 helix itself, and 47 when considering the ± 5 flanking amino acids. M2 was the most populated helix for disease variants compared to M1, M3, and M4 (χ^2 test p-value = 3.8e-7), and this effect was similar considering the TMH including the ± 5 flanking residues (χ^2 test p-value = 7.3e-7) (Figure 4).

Notably, as a trend, the variants in M2 were distributed throughout the helix, whereas in M1, which is the second most populated helix for disease variants, these were most common at the lipid-water interface and flanking regions particularly on the extracellular side (a peak of five disease variants at position −10. Also, the M1 has nine positions with no observed disease variants compared to four positions with no disease variants in the M2 (Figure 4c). M4 sustained fewer pathogenic variants, consistent with the lower conservation and higher tolerance for variation in gnomAD (Figure 1a, Figure S2).

4 | DISCUSSION

Here we report a novel de novo missense mutation in *GABRA2*. The phenotype of this case was EIEE, developmental delay, significant hypotonia, and congenital
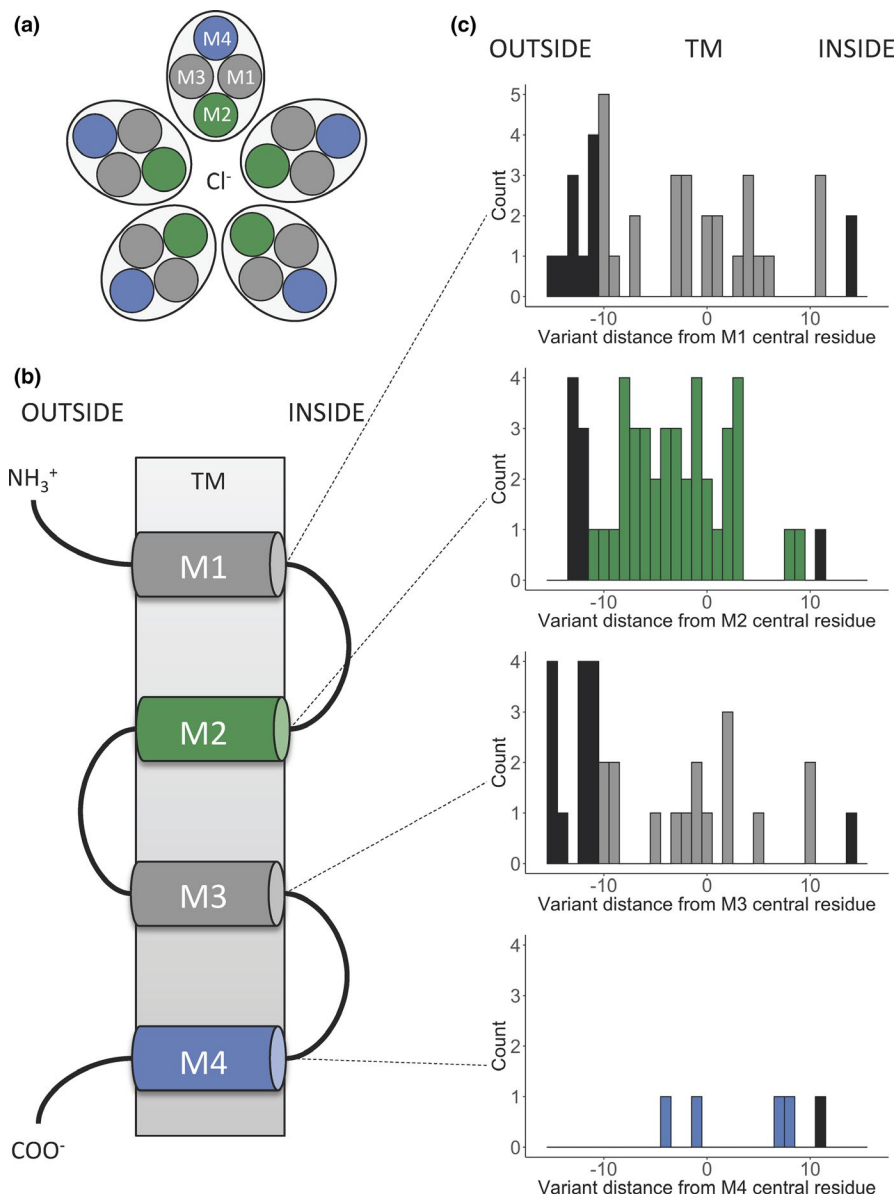

FIGURE 4 Distribution of disease variants along the TMH of Cys-loop receptors. (a) Top view schema of the TMH arrangement, considering the five subunits. (b) Simplified linear schema of the four helices of one subunit in the TM. (c) Positions of disease variants plotted as a distance in residues from the central TM residue in sequence. Negative positions are toward the "outside" (extracellular space), whereas positive positions are toward the "inside" (cytosol). The number of variants observed in the TMH was 86: M1 = 27, M2 = 39, M3 = 16, M4 = 4, and 122 including ± 5 flanking residues: M1 = 39, M2 = 47, M3 = 31, M4 = 5. In the histograms, disease variants in TMH are colored according to their position in the schema from Figure 4b, and disease variants in flanking regions are colored black. Duplicates in ClinVar and Humsavar are counted as one variant

nystagmus, similar to the previously reported individuals. The variant (Pro280Leu) was present in the −2' position of the channel pore (Bali & Akabas, 2007). This position is important for the ion-selectivity and desensitization of the ion channel, which are fundamental properties of most ligand-gated ion channels to change the conformation and limit the ion current flow, despite the neurotransmitter still being bound to the receptor (Gielen et al., 2015). We observed that the variant was in a highly conserved residue and the radius of the pore was narrowed at the gate in both closed and desensitized structures of the receptor. Having a residue like proline with a rigid side chain (or an alanine, observed in the β subunits, with a nonrigid but very small side chain) at the intracellular −2' position allows tight control of the gating upon neurotransmitter extracellular binding, exerting rigid body motion of the TMH, as can be observed in recent $GABA_A$ and Gly receptor structures (Hassaine et al., 2014; Hibbs & Gouaux, 2011; Duncan Laverty et al., 2017; Masiulis et al., 2019). Replacing the constraining proline with a leucine will permit changes in the backbone conformation (von Heijne, 1991). Moreover, ion-selectivity is determined by the −2' Pro in anion-selective channels, along with the −1' Ala (Keramidas, Moorhouse, Schofield, & Barry, 2004; Thompson et al., 2010), with no requirement for a charged side chain in the narrowest constriction.

Pathogenic missense mutations in *GABRA2* have been suggested to be compatible with both loss and gain-of-function (GOF) of the ion channel. Functional experiments on previously reported variants suggested to be compatible with a LOF (Maljevic et al., 2019), while a mutation in the activation gate (9') was associated with predominantly opened channels (Butler et al., 2018), therefore suggesting to result in the GOF of the receptor. The fact that opposing molecular effects result in the same disease could be explained by the dual role that *GABRA2* presents during development (Jenkins & Escayg, 2019), since early in life, $GABA_A$ receptors mediate excitation by depolarizing immature neurons in response to activation by GABA. The function of these receptors changes as the mature Cl^- gradient is established later in life, mediating inhibition by exerting hyperpolarization.

Mapping of the seven variants in *GABRA2* on the protein structure showed that they are located at key regions of the receptor. Six of the seven variants identified in *GABRA2* had equivalent pathogenic mutations in other Cys-loop receptors reported in the literature (Table 1), highlighting the importance of these regions. Although distinct phenotypes associated with the variants in Cys-loop receptors reflect their unique biological role, this family share a common structural topology conserved throughout evolution. Here, we show how variant interpretation by gathering together sequence, evolutionary, and structural information from homologous Cys-loop receptors can facilitate the characterization of novel candidate missense variants, especially in those cases where pathogenic mutations have already been characterized.

Furthermore, analysis of the distribution of previously reported pathogenic variants in the Cys-loop receptors showed that mutations are more common in the M2 segment than any other TMH, consistent with the importance of this helix in shaping the pore along the TM region. Also, the distribution of variants in M2 occurs throughout the helix, while disease variants in other helices that are more distant from the axis of the pore favor the water-lipid interface regions rather than the center of the TMH. Other clusters of pathogenic variants were observed in the M1 and M3 helices. M1 and M3 are more distant from the axis of the pore but play an important role in defining the inter-subunit interaction interfaces (Ducan Laverty et al., 2017). In contrast, M4 has fewer pathogenic variants, consistent with this region being less conserved and more tolerant to variation in gnomAD (Figure 1 and Figure S2). Although mutations in these helices have been studied and demonstrated to influence channel gating kinetics, agonist sensitivity, and create spontaneous opening channels in different members of the Cys-loop receptors (Chang & Weiss, 1999; Chang, Wu, Zhang, & Huang, 2009), their distribution in the protein structure across the different members of the family has never been assessed. Our results provide a better understanding of the structural location of pathogenic variants in the TMH of Cys-loop receptors, facilitating further interpretation of novel candidate disease-causing mutations.

Herein, we present a novel de novo missense variant in *GABRA2* in a patient with EIEE and perform protein structural analysis of the previously reported and the novel variants. Our results highlight the importance of performing structural analysis of missense mutations in *GABRA2*, in order to provide a more accurate insight into the etiology of the disease that might also lead to opportunities for personalized treatments.

CONFLICT OF INTEREST STATEMENT
The authors declare that they have no competing interests.

ACKNOWLEDGMENTS

AUTHOR CONTRIBUTIONS

DATA AVAILABILITY STATEMENT

Sequence data for the trio have been deposited at the European Genome-Phenome Archive (EGAD00001004522).

ORCID

Alba Sanchis-Juan 🔟 https://orcid.org/0000-0003-2788-5497

REFERENCES

Adzhubei, I., Jordan, D. M., & Sunyaev, S. R. (2013). Predicting functional effect of human missense mutations using PolyPhen-2. _Current Protocols in Human Genetics., Chapter 7_, Unit7.20. https://doi.org/10.1002/0471142905.hg0720s76

Akk, G., Li, P., Bracamontes, J., Reichert, D. E., Covey, D. F., & Steinbach, J. H. (2008). Mutations of the GABA-A receptor alpha1 subunit M1 domain reveal unexpected complexity for modulation by neuroactive steroids. _Molecular Pharmacology_, _74_(3), 614–627. https://doi.org/10.1124/mol.108.048520

Al-Owain, M., Colak, D., Al-Bakheet, A., Al-Hashmi, N., Shuaib, T., Al-Hemidan, A., … Kaya, N. (2012). Novel mutation in GLRB in a large family with hereditary hyperekplexia. _Clinical Genetics_, _81_(5), 479–484. https://doi.org/10.1111/j.1399-0004.2011.01661.x

Aridon, P., Marini, C., Di Resta, C., Brilli, E., De Fusco, M., Politi, F., … Casari, G. (2006). Increased sensitivity of the neuronal nicotinic receptor alpha 2 subunit causes familial epilepsy with nocturnal wandering and ictal fear. _American Journal of Human Genetics_, _79_(2), 342–350. https://doi.org/10.1086/506459

Baker, N. A., Sept, D., Joseph, S., Holst, M. J., & McCammon, J. A. (2001). Electrostatics of nanosystems: Application to microtubules and the ribosome. _Proceedings of the National Academy of Sciences USA_, _98_(18), 10037–10041. https://doi.org/10.1073/pnas.181342398

Bali, M., & Akabas, M. H. (2007). The location of a closed channel gate in the GABAA receptor channel. _Journal of General Physiology_, _129_(2), 145–159. https://doi.org/10.1085/jgp.200609639

Berman, H. M., Westbrook, J., Feng, Z., Gilliland, G., Bhat, T. N., Weissig, H., … Bourne, P. E. (2000). The protein data bank. _Nucleic Acids Research_, _28_(1), 235–242. https://doi.org/10.1093/nar/28.1.235

Butler, K. M., Moody, O. A., Schuler, E., Coryell, J., Alexander, J. J., Jenkins, A., & Escayg, A. (2018). De novo variants in GABRA2 and GABRA5 alter receptor function and contribute to early-onset epilepsy. _Brain_, https://doi.org/10.1093/brain/awy171

Carss, K. J., Arno, G., Erwood, M., Stephens, J., Sanchis-Juan, A., Hull, S., … Yu, P. (2017). Comprehensive rare variant analysis via Whole-Genome sequencing to determine the molecular pathology of inherited retinal disease. _American Journal of Human Genetics_, _100_(1), 75–90. https://doi.org/10.1016/j.ajhg.2016.12.003

Chang, Y., & Weiss, D. S. (1999). Allosteric activation mechanism of the alpha 1 beta 2 gamma 2 gamma-aminobutyric acid type A receptor revealed by mutation of the conserved M2 leucine. _Biophysical Journal_, _77_(5), 2542–2551.

Chang, Y.-C., Wu, W., Zhang, J.-L., & Huang, Y. (2009). Allosteric activation mechanism of the cys-loop receptors. _Acta Pharmacologica Sinica_, _30_(6), 663–672. https://doi.org/10.1038/aps.2009.51

Chen, X., Schulz-Trieglaff, O., Shaw, R., Barnes, B., Schlesinger, F., Källberg, M., … Saunders, C. T. (2016). Manta: Rapid detection of structural variants and indels for germline and cancer sequencing applications. _Bioinformatics_, _32_(8), 1220–1222. https://doi.org/10.1093/bioinformatics/btv710

Cho, Y.-W., Motamedi, G. K., Laufenberg, I., Sohn, S.-I., Lim, J.-G., Lee, H., … Steinlein, O. K. (2003). A Korean kindred with autosomal dominant nocturnal frontal lobe epilepsy and mental retardation. _Archives of Neurology_, _60_(11), 1625–1632. https://doi.org/10.1001/archneur.60.11.1625

Conti, V., Aracri, P., Chiti, L., Brusco, S., Mari, F., Marini, C., … Guerrini, R. (2015). Nocturnal frontal lobe epilepsy with paroxysmal arousals due to CHRNA2 loss of function. _Neurology_, _84_(15), 1520–1528. https://doi.org/10.1212/WNL.0000000000001471

Davydov, E. V., Goode, D. L., Sirota, M., Cooper, G. M., Sidow, A., & Batzoglou, S. (2010). Identifying a high fraction of the human genome to be under selective constraint using GERP++. _PLoS Computational Biology_, _6_(12), e1001025. https://doi.org/10.1371/journal.pcbi.1001025

del Giudice, E. M., Coppola, G., Bellini, G., Cirillo, G., Scuccimarra, G., & Pascotto, A. (2001). A mutation (V260M) in the middle of the M2 pore-lining domain of the glycine receptor causes hereditary hyperekplexia. _European Journal of Human Genetics_, _9_(11), 873–876. https://doi.org/10.1038/sj.ejhg.5200729

Delano, W. L. (2002). _The PyMOL Molecular Graphics System, Version 2.0_. Schrödinger LLC.

Dobson, L., Meszaros, B., & Tusnady, G. E. (2018). Structural principles governing disease-causing germline mutations. _Journal of Molecular Biology_, _430_(24), 4955–4970. https://doi.org/10.1016/j.jmb.2018.10.005

Dolinsky, T. J., Czodrowski, P., Li, H., Nielsen, J. E., Jensen, J. H., Klebe, G., & Baker, N. A. (2007). PDB2PQR: Expanding and upgrading automated preparation of biomolecular structures for molecular simulations. _Nucleic Acids Research_, _35_(Web Server), W522–525. https://doi.org/10.1093/nar/gkm276

Edenberg, H. J., Dick, D. M., Xuei, X., Tian, H., Almasy, L., Bauer, L. O., … Begleiter, H. (2004). Variations in GABRA2, encoding the alpha 2 subunit of the GABA(A) receptor, are associated with alcohol dependence and with brain oscillations. _American Journal of Human Genetics_, _74_(4), 705–714. https://doi.org/10.1086/383283

Farnaes, L., Nahas, S. A., Chowdhury, S., Nelson, J., Batalov, S., Dimmock, D. M., … Investigators, R. (2017). Rapid whole-genome sequencing identifies a novel GABRA1 variant associated with West syndrome. _Cold Spring Harbor Molecular Case Studies_, _3_(5), https://doi.org/10.1101/mcs.a001776

Follwaczny, P., Schieweck, R., Riedemann, T., Demleitner, A., Straub, T., Klemm, A. H., … Kiebler, M. A. (2017). Pumilio2-deficient mice show a predisposition for epilepsy. *Disease Models & Mechanisms*, *10*(11), 1333–1342. https://doi.org/10.1242/dmm.029678

Gielen, M., Thomas, P., & Smart, T. G. (2015). The desensitization gate of inhibitory Cys-loop receptors. *Nature Communications*, *6*, 6829. https://doi.org/10.1038/ncomms7829

Gomez, C. M., Maselli, R., Gammack, J., Lasalde, J., Tamamizu, S., Cornblath, D. R., … Kuncl, R. W. (1996). A beta-subunit mutation in the acetylcholine receptor channel gate causes severe slow-channel syndrome. *Annals of Neurology*, *39*(6), 712–723. https://doi.org/10.1002/ana.410390607

Gonzalez-Nunez, V. (2015). Role of gabra2, GABAA receptor alpha-2 subunit, in CNS development. *Biochemistry and Biophysics Reports*, *3*, 190–201. https://doi.org/10.1016/j.bbrep.2015.08.003

Hamdan, F. F., Myers, C. T., Cossette, P., Lemay, P., Spiegelman, D., Laporte, A. D., … Michaud, J. L. (2017). High rate of recurrent De Novo mutations in developmental and epileptic encephalopathies. *American Journal of Human Genetics*, *101*(5), 664–685. https://doi.org/10.1016/j.ajhg.2017.09.008

Hassaine, G., Deluz, C., Grasso, L., Wyss, R., Tol, M. B., Hovius, R., … Nury, H. (2014). X-ray structure of the mouse serotonin 5-HT3 receptor. *Nature*, *512*(7514), 276–281. https://doi.org/10.1038/nature13552

Havrilla, J. M., Pedersen, B. S., Layer, R. M., & Quinlan, A. R. (2018). A map of constrained coding regions in the human genome. *Nature Genetics*, *51*(1), 88–95. https://doi.org/10.1038/s41588-018-0294-6

Hawkins, N. A., Zachwieja, N. J., Miller, A. R., Anderson, L. L., & Kearney, J. A. (2016). Fine mapping of a dravet syndrome modifier locus on mouse chromosome 5 and candidate gene analysis by RNA-Seq. *PLoS Genetics*, *12*(10), e1006398. https://doi.org/10.1371/journal.pgen.1006398

Hernandez, C. C., Kong, W., Hu, N., Zhang, Y., Shen, W., Jackson, L., … Macdonald, R. L. (2017). Altered channel conductance states and gating of GABA receptors by a pore mutation linked to dravet syndrome. *eNeuro*, *4*(1), 1–33. https://doi.org/10.1523/ENEURO.0251-16.2017

Hibbs, R. E., & Gouaux, E. (2011). Principles of activation and permeation in an anion-selective Cys-loop receptor. *Nature*, *474*(7349), 54–60. https://doi.org/10.1038/nature10139

Hirose, S. (2014). Mutant GABA(A) receptor subunits in genetic (idiopathic) epilepsy. *Progress in Brain Research*, *213*, 55–85. https://doi.org/10.1016/B978-0-444-63326-2.00003-X

Hirose, S., Iwata, H., Akiyoshi, H., Kobayashi, K., Ito, M., Wada, K., … Mitsudome, A. (1999). A novel mutation of CHRNA4 responsible for autosomal dominant nocturnal frontal lobe epilepsy. *Neurology*, *53*(8), 1749–1753. https://doi.org/10.1212/WNL.53.8.1749

Hwang, S.-K., Makita, Y., Kurahashi, H., Cho, Y.-W., & Hirose, S. (2011). Autosomal dominant nocturnal frontal lobe epilepsy: A genotypic comparative study of Japanese and Korean families carrying the CHRNA4 Ser284Leu mutation. *Journal of Human Genetics*, *56*(8), 609–612. https://doi.org/10.1038/jhg.2011.69

International League Against Epilepsy Consortium on Complex Epilepsies (2014). Genetic determinants of common epilepsies: A meta-analysis of genome-wide association studies. *The Lancet Neurology*, *13*(9), 893–903. https://doi.org/10.1016/S1474-4422(14)70171-1

International League Against Epilepsy Consortium on Complex Epilepsies (2018). Genome-wide mega-analysis identifies 16 loci and highlights diverse biological mechanisms in the common epilepsies. *Nature Communications*, *9*(1), 5269. https://doi.org/10.1038/s41467-018-07524-z

James, V. M., Bode, A., Chung, S.-K., Gill, J. L., Nielsen, M., Cowan, F. M., … Harvey, R. J. (2013). Novel missense mutations in the glycine receptor β subunit gene (GLRB) in startle disease. *Neurobiology of Diseases*, *52*, 137–149. https://doi.org/10.1016/j.nbd.2012.12.001

Jenkins, A., & Escayg, A. (2019). Reply: Novel GABRA2 variants in epileptic encephalopathy and intellectual disability with seizures. *Brain*, *142*(5), e16. https://doi.org/10.1093/brain/awz086

Katoh, K., & Standley, D. M. (2013). MAFFT multiple sequence alignment software version 7: Improvements in performance and usability. *Molecular Biology and Evolution*, *30*(4), 772–780. https://doi.org/10.1093/molbev/mst010

Keramidas, A., Moorhouse, A. J., Schofield, P. R., & Barry, P. H. (2004). Ligand-gated ion channels: Mechanisms underlying ion selectivity. *Progress in Biophysics and Molecular Biology*, *86*(2), 161–204. https://doi.org/10.1016/j.pbiomolbio.2003.09.002

Kircher, M., Witten, D. M., Jain, P., O'Roak, B. J., Cooper, G. M., & Shendure, J. (2014). A general framework for estimating the relative pathogenicity of human genetic variants. *Nature Genetics*, *46*(3), 310–315. https://doi.org/10.1038/ng.2892

Kodera, H., Ohba, C., Kato, M., Maeda, T., Araki, K., Tajima, D., … Matsumoto, N. (2016). De novo GABRA1 mutations in Ohtahara and West syndromes. *Epilepsia*, *57*(4), 566–573. https://doi.org/10.1111/epi.13344

Kurahashi, H., & Hirose, S. (2002). Autosomal Dominant Nocturnal Frontal Lobe Epilepsy. In M. P. Adam, H. H. Ardinger, R. A. Pagon, S. E. Wallace, L. J. H. Bean, K. Stephens, & A. Amemiya (Eds.), *GeneReviews®*. Seattle (WA): University of Washington, Seattle.

Landrum, M. J., Lee, J. M., Benson, M., Brown, G. R., Chao, C., Chitipiralla, S., … Maglott, D. R. (2018). ClinVar: Improving access to variant interpretations and supporting evidence. *Nucleic Acids Research*, *46*(D1), D1062–D1067. https://doi.org/10.1093/nar/gkx1153

Laverty, D., Desai, R., Uchanski, T., Masiulis, S., Stec, W. J., Malinauskas, T., … Aricescu, A. R. (2019). Cryo-EM structure of the human alpha1beta3gamma2 GABAA receptor in a lipid bilayer. *Nature*, *565*(7740), 516–520. https://doi.org/10.1038/s41586-018-0833-4

Laverty, D., Thomas, P., Field, M., Andersen, O. J., Gold, M. G., Biggin, P. C., … Smart, T. G. (2017). Crystal structures of a GABAA-receptor chimera reveal new endogenous neurosteroid-binding sites. *Nature Structural & Molecular Biology*, *24*(11), 977–985. https://doi.org/10.1038/nsmb.3477

Lek, M., Karczewski, K. J., Minikel, E. V., Samocha, K. E., Banks, E., Fennell, T., … MacArthur, D. G. (2016). Analysis of protein-coding genetic variation in 60,706 humans. *Nature*, *536*(7616), 285–291. https://doi.org/10.1038/nature19057

Lester, H. A., Dibas, M. I., Dahan, D. S., Leite, J. F., & Dougherty, D. A. (2004). Cys-loop receptors: New twists and turns. *Trends in Neurosciences*, *27*(6), 329–336. https://doi.org/10.1016/j.tins.2004.04.002

Maljevic, S., Keren, B., Aung, Y. H., Forster, I. C., Mignot, C., Buratti, J., … Nava, C. (2019). Novel GABRA2 variants in epileptic encephalopathy and intellectual disability with seizures. *Brain*, *142*(5), e15. https://doi.org/10.1093/brain/awz079

Martin, A. J. M., Vidotto, M., Boscariol, F., Di Domenico, T., Walsh, I., & Tosatto, S. C. E. (2011). RING: Networking interacting residues, evolutionary information and energetics in protein structures.

Bioinformatics, *27*(14), 2003–2005. https://doi.org/10.1093/bioinformatics/btr191

Masiulis, S., Desai, R., Uchański, T., Serna Martin, I., Laverty, D., Karia, D., … Aricescu, A. R. (2019). GABAA receptor signalling mechanisms revealed by structural pharmacology. *Nature*, *565*(7740), 454–459. https://doi.org/10.1038/s41586-018-0832-5

McLachlan, A. (1982). Rapid comparison of protein structures. *Acta Crystallographica Section A*, *38*(6), 871–873. https://doi.org/10.1107/S0567739482001806

McLaren, W., Gil, L., Hunt, S. E., Riat, H. S., Ritchie, G. R. S., Thormann, A., … Cunningham, F. (2016). The ensembl variant effect predictor. *Genome Biology*, *17*(1), 122. https://doi.org/10.1186/s13059-016-0974-4

Mihic, S. J., Ye, Q., Wick, M. J., Koltchine, V. V., Krasowski, M. D., Finn, S. E., … Harrison, N. L. (1997). Sites of alcohol and volatile anaesthetic action on GABA(A) and glycine receptors. *Nature*, *389*(6649), 385–389. https://doi.org/10.1038/38738

Myers, C. T., McMahon, J. M., Schneider, A. L., Petrovski, S., Allen, A. S., Carvill, G. L., … Mefford, H. C. (2016). De Novo Mutations in SLC1A2 and CACNA1A Are Important Causes of Epileptic Encephalopathies. *American Journal of Human Genetics*, *99*(2), 287–298. https://doi.org/10.1016/j.ajhg.2016.06.003

Ng, P. C., & Henikoff, S. (2003). SIFT: Predicting amino acid changes that affect protein function. *Nucleic Acids Research*, *31*(13), 3812–3814. https://doi.org/10.1093/nar/gkg509

Nys, M., Kesters, D., & Ulens, C. (2013). Structural insights into Cys-loop receptor function and ligand recognition. *Biochemical Pharmacology*, *86*(8), 1042–1053. https://doi.org/10.1016/j.bcp.2013.07.001

Olsen, R. W. (2018). GABAA receptor: Positive and negative allosteric modulators. *Neuropharmacology*, *136*(Pt A), 10–22. https://doi.org/10.1016/j.neuropharm.2018.01.036

Orenstein, N., Goldberg-Stern, H., Straussberg, R., Bazak, L., Weisz Hubshman, M., Kropach, N., … Basel-Salmon, L. (2018). A de novo GABRA2 missense mutation in severe early-onset epileptic encephalopathy with a choreiform movement disorder. *European Journal of Paediatric Neurology*, *22*(3), 516–524. https://doi.org/10.1016/j.ejpn.2017.12.017

Ortells, M. O., & Lunt, G. G. (1995). Evolutionary history of the ligand-gated ion-channel superfamily of receptors. *Trends in Neurosciences*, *18*(3), 121–127. https://doi.org/10.1016/0166-2236(95)93887-4

Pellegrini-Calace, M., Maiwald, T., & Thornton, J. M. (2009). PoreWalker: A novel tool for the identification and characterization of channels in transmembrane proteins from their three-dimensional structure. *PLoS Computational Biology*, *5*(7), e1000440. https://doi.org/10.1371/journal.pcbi.1000440

Prenosil, G. A., Schneider Gasser, E. M., Rudolph, U., Keist, R., Fritschy, J.-M., & Vogt, K. E. (2006). Specific subtypes of GABAA receptors mediate phasic and tonic forms of inhibition in hippocampal pyramidal neurons. *Journal of Neurophysiology*, *96*(2), 846–857. https://doi.org/10.1152/jn.01199.2005

Raczy, C., Petrovski, R., Saunders, C. T., Chorny, I., Kruglyak, S., Margulies, E. H., … Tanner, S. W. (2013). Isaac: Ultra-fast whole-genome secondary analysis on Illumina sequencing platforms. *Bioinformatics*, *29*(16), 2041–2043. https://doi.org/10.1093/bioinformatics/btt314

Roller, E., Ivakhno, S., Lee, S., Royce, T., & Tanner, S. (2016). Canvas: Versatile and scalable detection of copy number variants.

Bioinformatics, *32*(15), 2375–2377. https://doi.org/10.1093/bioinformatics/btw163

Sanchis-Juan, A., Stephens, J., French, C. E., Gleadall, N., Mégy, K., Penkett, C., … Carss, K. J. (2018). Complex structural variants in Mendelian disorders: Identification and breakpoint resolution using short- and long-read genome sequencing. *Genome Medicine*, *10*(1), 95. https://doi.org/10.1186/s13073-018-0606-6

Sauguet, L., Poitevin, F., Murail, S., Van Renterghem, C., Moraga-Cid, G., Malherbe, L., … Delarue, M. (2013). Structural basis for ion permeation mechanism in pentameric ligand-gated ion channels. *EMBO Journal*, *32*(5), 728–741. https://doi.org/10.1038/emboj.2013.17

Saul, B., Kuner, T., Sobetzko, D., Brune, W., Hanefeld, F., Meinck, H. M., & Becker, C. M. (1999). Novel GLRA1 missense mutation (P250T) in dominant hyperekplexia defines an intracellular determinant of glycine receptor channel gating. *Journal of Neuroscience*, *19*(3), 869–877.

Schymkowitz, J., Borg, J., Stricher, F., Nys, R., Rousseau, F., & Serrano, L. (2005). The FoldX web server: An online force field. *Nucleic Acids Research*, *33*(Web Server), W382–388. https://doi.org/10.1093/nar/gki387

Shiang, R., Ryan, S. G., Zhu, Y. Z., Hahn, A. F., O'Connell, P., & Wasmuth, J. J. (1993). Mutations in the alpha 1 subunit of the inhibitory glycine receptor cause the dominant neurologic disorder, hyperekplexia. *Nature Genetics*, *5*(4), 351–358. https://doi.org/10.1038/ng1293-351

Sigel, E., & Steinmann, M. E. (2012). Structure, function, and modulation of GABA(A) receptors. *Journal of Biological Chemistry*, *287*(48), 40224–40231. https://doi.org/10.1074/jbc.R112.386664

Steinlein, O. K., Hoda, J. C., Bertrand, S., & Bertrand, D. (2012). Mutations in familial nocturnal frontal lobe epilepsy might be associated with distinct neurological phenotypes. *Seizure*, *21*(2), 118–123. https://doi.org/10.1016/j.seizure.2011.10.003

Stephenson, J. D., Laskowski, R. A., Nightingale, A., Hurles, M. E., & Thornton, J. M. (2019). VarMap: A web tool for mapping genomic coordinates to protein sequence and structure and retrieving protein structural annotations. *Bioinformatics*, *35*(22), 4854–4856. https://doi.org/10.1093/bioinformatics/btz48210.1093/bioinformatics/btz482

Strac, D. S., Erjavec, G. N., Perkovic, M. N., Sviglin, K. N., Borovecki, F., & Pivac, N. (2015). Association of GABAA receptor α2 subunit gene (GABRA2) with alcohol dependence-related aggressive behavior. *Progress in Neuro-Psychopharmacology and Biological Psychiatry*, *63*, 119–125. https://doi.org/10.1016/j.pnpbp.2015.06.010

Thompson, A. J., Lester, H. A., & Lummis, S. C. R. (2010). The structural basis of function in Cys-loop receptors. *Quarterly Reviews of Biophysics*, *43*(04), 449–499. https://doi.org/10.1017/s0033583510000168

Tian, H., Chen, H.-J., Cross, T. H., & Edenberg, H. J. (2005). Alternative splicing and promoter use in the human GABRA2 gene. *Molecular Brain Research*, *137*(1–2), 174–183. https://doi.org/10.1016/j.molbrainres.2005.03.001

UniProt, C. (2019). UniProt: A worldwide hub of protein knowledge. *Nucleic Acids Research*, *47*(D1), D506–D515. https://doi.org/10.1093/nar/gky1049

von Heijne, G. (1991). Proline kinks in transmembrane α-helices. *Journal of Molecular Biology*, *218*(3), 499–503. https://doi.org/10.1016/0022-2836(91)90695-3

Walters, R. J., Hadley, S. H., Morris, K. D., & Amin, J. (2000). Benzodiazepines act on GABAA receptors via two distinct and separable mechanisms. *Nature Neuroscience*, *3*(12), 1274–1281. https://doi.org/10.1038/81800

Wang, D. D., & Kriegstein, A. R. (2009). Defining the role of GABA in cortical development. *Journal of Physiology*, *587*(Pt 9), 1873–1879. https://doi.org/10.1113/jphysiol.2008.167635

Wang, H.-L., Milone, M., Ohno, K., Shen, X.-M., Tsujino, A., Batocchi, A. P., … Sine, S. M. (1999). Acetylcholine receptor M3 domain: Stereochemical and volume contributions to channel gating. *Nature Neuroscience*, *2*(3), 226–233. https://doi.org/10.1038/6326

Waterhouse, A. M., Procter, J. B., Martin, D. M. A., Clamp, M., & Barton, G. J. (2009). Jalview Version 2–a multiple sequence alignment editor and analysis workbench. *Bioinformatics*, *25*(9), 1189–1191. https://doi.org/10.1093/bioinformatics/btp033

SUPPORTING INFORMATION

Additional supporting information may be found online in the Supporting Information section.

How to cite this article: Sanchis-Juan A, Hasenahuer MA, Baker JA, et al. Structural analysis of pathogenic missense mutations in *GABRA2* and identification of a novel de novo variant in the desensitization gate. *Mol Genet Genomic Med*. 2020;00:e1106. https://doi.org/10.1002/mgg3.1106